# $Z_2$ and energy dependence of range distributions and stopping powers for nitrogen ions in solids

David J. Land, Donald G. Simons, James G. Brennan,* and Matt D. Brown
*Naval Surface Weapons Center, White Oak, Silver Spring, Maryland 20910*
(Received 13 November 1979)

Range distributions of nitrogen ions implanted in solid targets have been studied as a function of target material and projectile energy and for both atomic- and molecular-ion species. These profiles were determined by a nuclear resonance reaction technique in which the $^{14}N(p,\gamma)^{15}O$ reaction at 1058 keV was used. At a single energy of 800 keV, $^{14}N^+$ ions were implanted in 24 elemental targets from carbon through lead. From these range distributions electronic stopping powers were inferred which show the familiar periodic structure with target atomic number. For three targets, iron, nickel, and zirconium, the energy dependence of the range distributions was studied for incident $^{14}N^+$ ions from 200 to 2000 keV. The data suggest that the electronic stopping power has the same energy dependence for each target and is consistent with being proportional to velocity. For these three targets and for gold also, the range distributions were determined for both atomic and molecular nitrogen-ion beams of equal energy per atom. The data suggest that at higher particle energies the molecular beam gives rise to slightly more shallow distributions.

## I. INTRODUCTION

The problem of understanding and predicting the range distributions of heavy ions in matter continues to draw considerable attention because of numerous practical applications. Particularly important examples include the use of ion implantation in device fabrication and in studies of reactor wall damage. As part of the overall problem of estimating distributions through the use of theoretical models, knowledge of the stopping power is crucial. In an extensive experimental and theoretical program at the Naval Surface Weapons Center,[1-6] we have been studying the range distributions and stopping powers of heavy ions at low velocity (velocity comparable to the velocity of the outer atomic electrons). Our program has been based on numerous experimental measurements of the range distributions of nitrogen ions implanted in solid target materials. From these experimentally determined range distributions we inferred electronic stopping powers. Using these experimental results as a guide, two of the present authors[5,6] have developed a general theoretical modeling for the low-velocity electronic stopping power applicable to all combinations of incident ions and target atoms.

In previous work we have measured the range distributions of 800-keV $^{14}N^+$ ions implanted in solid target materials from titanium ($Z_2 = 22$) to germanium ($Z_2 = 32$).[1] The range distributions were determined by a nuclear-resonance reaction technique in which the $^{14}N(p,\gamma)^{15}O$ reaction at 1058 keV was used. From these measurements we obtained three moments of the range distributions; the first two moments were related to the nuclear and electronic stopping through the use of the Lindhard-Scharff-Schiött (LSS) transport theory.[7] From the first moment of the distribution, the projected range, the electronic stopping power was inferred under the assumption of velocity-proportional electronic stopping. We found that the electronic stopping displays a periodic structure as a function of target atomic number for nitrogen projectiles similar to the behavior obtained for lighter projectiles $p$, He and Li,[8] and for incident projectiles at constant velocity in both solid and gaseous targets.[9]

A significant result of that work was the finding that the range straggling, when calculated from LSS theory, using the experimentally inferred values for electronic stopping, agrees much more closely with the data than when calculated using the Lindhard-Scharff (LS) values for the electronic stopping.[10]

In the present work we have extended these results in several ways. First, we have added many elements as target materials above and below our earlier $Z_2$ region. The new region includes an extensive series of elements from zirconium ($Z_2 = 40$) to tellurium ($Z_2 = 52$), as well as carbon and silicon targets below this region and tantalum, gold, and lead targets above. Second, we have chosen three targets, iron, nickel, and zirconium, for a study of the energy dependence of the range distributions for incident nitrogen ions from 200 to 2000 keV. These targets were chosen to have one near a maximum in the stopping-power curve, one near a minimum, and one near a midpoint in order to see if the energy dependence of $S_e$ depends on the target material. Third, for these targets and for gold we have determined range distributions for incident beams of atomic nitrogen $N^+$ and of molecular nitrogen $N_2^+$ at two energies,

200 and 400 keV per atom. This study was done in order to see if the distributions depend on the atomic or molecular nature of the incident beam. Many implantations are performed using molecular beams and for these this question is quite relevant. In addition, recent experimental work involving MeV particle clusters as projectiles shows differences in the energy and angular distribution of the constituents upon emerging from thin foils.[11]

In general, the experimental procedures and techniques of the data analysis are the same as those employed in our earlier work[1] and a detailed description of the methods is not repeated here. However, there is one significant difference. It was found that the resonance energy for the $^{14}N(p,\gamma)^{15}O$ nuclear reaction of 1061 keV which we had been using is too high by 3 keV. More accurate values for the resonance energy and width are 1058 and 4.0 keV, respectively. These values have been obtained in separate experiments by Nero[12] and by the present authors[13] and have been adopted in this work. In addition, we are now using the recently compiled proton stopping values of Andersen and Ziegler.[14] We have therefore reanalyzed all our data using the new resonance parameters and the Andersen-Ziegler proton stopping and present in this paper all our results for the nitrogen range distributions and electronic stopping powers.

In studies reported elsewhere,[4] we have obtained range distributions for $N^+$ and $N_2^+$ ions implanted at lower energies, 25 to 150 keV per atom. To show a complete picture of the energy dependence of the nitrogen range distributions, we also include these results here. This paper thus serves as a summary report of our entire program.

## II. EXPERIMENTAL PROCEDURES AND DATA ANALYSIS

The nitrogen implantations were performed using the 2.5-MV Van de Graaff accelerator at the Naval Surface Weapons Center. Fluences were chosen such that the maximum implant density is never greater than 10% of the target atomic density. A typical fluence for an 800-keV implant is $10^{17}$ atoms/cm$^2$. Sample comparisons of these implant distributions with distributions having one-tenth this fluence showed no significant fluence dependence.

The physical form of the targets was chosen by availability and $(p,\gamma)$ backgrounds. Polycrystalline bulk samples were used for V, Mn, Fe, Co, Ni, Cu, Zn, Nb, Mo, Rh, Ag, Cd, In, Sn, Au, and Pb. Those targets which had rough surfaces were mechanically polished with 600 grit SiC. For those cases with large $(p,\gamma)$ backgrounds (Ti, Cr and Zn) or where bulk sample was not available (Te), thin targets were prepared by vacuum evaporation onto a low background backing (Ta or Ni). These targets were required to be at least 3 $\mu$m thick. This thickness was sufficient to stop all of the $^{14}N$ ions but thin enough to reduce the high $\gamma$-ray backgrounds. Two targets (Si and Ge) were single crystals. These targets were mounted with their crystal axis a few degrees with respect to the beam to minimize the chance of channeling both during implantation and $(p,\gamma)$ probing. These two targets were the only targets which were not rotated in the beam during implantation. The carbon target was a vitreous carbon used to assure a nonporous, polished surface. All targets were at least 99.9% pure. In the cases of low-melting-point targets (Cd, In, Sn and Te), care was taken to use low beam currents during implantation and probing to ensure that they would not overheat or melt.

Concentration distributions for the implanted nitrogen ions were determined by measuring the $\gamma$-ray yield induced by incident protons as a function of proton energy. The $^{14}N(p,\gamma)^{15}O$ nuclear resonance reaction at 1058 keV was used to unfold from the measured yield the effects of proton straggling in the target, the finite width of the nuclear resonance (4.0 keV), and the width of the incident beam (about 1.2 keV). The range distributions were characterized by a specific analytic form, a split-Gaussian curve. This curve consists of two half-Gaussians of different widths, $\Delta R_-$ and $\Delta R_+$, joined at the peak position, $R_{\text{peak}}$.[15] The three parameters of this distribution, $R_{\text{peak}}$, $\Delta R_-$, and $\Delta R_+$, were determined by varying them until the $\gamma$-ray yield calculated from the assumed range distribution matched the experimentally measured yield in a least-squares sense.

With the exception of Monte Carlo calculations, theoretical determinations for the range distribution are invariably given by the first few moments only, and hence we should express the distributions obtained by our procedure in terms of their moments. One can readily find for the first three moments, the projected range $R_p$, the straggling in projected range $\Delta R_p$, and the skewness $\Delta R_{3p}$, the relations

$$\begin{aligned} R_p &= R_{\text{peak}} + 0.798(\Delta R_+ + \Delta R_-)\,, \\ \Delta R_p^2 &= 0.363(\Delta R_+^2 + \Delta R_-^2) + 0.752\Delta R_+\Delta R_-)\,, \\ \Delta R_{3p}^3 &= 0.601(\Delta R_+ - \Delta R_-)(\Delta R_p^2 + 0.329\Delta R_+\Delta R_-)\,, \end{aligned} \tag{1}$$

in terms of the parameters of the split-Gaussian distribution. However, because of the restricted nature of the assumed asymptotic behavior for this distribution, high-order moments rapidly become meaningless if compared with those for the physical distribution. In fact, the third moment of

the split-Gaussian cannot exceed in absolute value a number which is about 1, and this in in gross disagreement with more detailed analysis presented by Winterbon[16] which shows that the third moment can take values −2 to −3 for the projectile-target combinations studied here. Thus, while the split-Gaussian form provides a convenient and useful representation for the range distribution, we take only the first two moments to be quantitatively meaningful with the third moment indicating only the sign of the skewness. However, experience has shown us that, given a measured $\gamma$-ray distribution, the inferred values particularly for the projected range and for the straggling also tend to be independent of the deconvolution technique employed and so we have confidence in these quantities.

The calculations were performed with the use of LSS transport theory. All implants in this study are sufficiently deep that the use of the LSS transport theory as an infinite-medium theory is allowable. The effects of reflection of ions from the front surface is not important here. This conclusion is not true for low-energy implants. In particular, for the nitrogen implants we have studied at energies from 25–150 keV,[4] we found a buildup of N atoms at the front surface to form a peak which became more pronounced as the implant energy decreased. This behavior is similar to that found by Luomajärvi *et al.* in their studies of low-energy $^{15}$N implantations.[17]

From the projected range of the concentration distributions we infer the electronic stopping power. The projected range for projectiles with initial energy $E$ is related to the nuclear and electronic stopping powers within the LSS transport theory[7] by the expression

$$R_p(E) = \int_0^E \frac{dE'}{NS_{\rm tr}(E')} \times \exp\left(-\int_{E'}^{E} \frac{dE''}{\lambda_{\rm tr}(E'')NS_{\rm tr}(E'')}\right), \qquad (2)$$

where

$$S_{\rm tr}(E) = S_e(E) + S_{n,\rm tr}(E)\,,$$

$$S_{n,\rm tr}(E) = \int d\sigma_n T\,\cos\phi\,,$$

$$\lambda_{\rm tr}^{-1}(E) = N\int d\sigma_n(1-\cos\phi)\,,$$

$N$ is the atomic density, and $d\sigma_n$ is the differential cross section for energy transfer $T$ to the target nucleus from the projectile scattered at the laboratory angle $\phi$. For our studies of the 800-keV implants the electronic stopping is determined by assuming it is proportional to the projectile velocity $v$:

$$S_e(E) = A(v/v_0) = A(E/E_0)^{1/2}\,,$$

where $E_0$ is the energy for which $v = v_0$ and $v_0$ is the Bohr velocity $e^2/\hbar$. The constant $A$ is determined so that values of $R_p$ calculated from Eq. (2) above reproduce the measured values in a least-squares sense. The values for the range straggling $\Delta R_p$, corresponding to this inferred value for $S_e$ can now be calculated.

While the large angle scattering which results from the nuclear stopping exerts a significant effect on $R_p$ in this energy region, we have shown in our previous work[1] that calculated values of $R_p$ and $\Delta R_p$ are rather insensitive to the magnitude of the total cross sections governing the nuclear stopping power. On the other hand, $R_p$ is quite sensitive to the magnitude of the electronic stopping power. Thus we conclude that our procedure constitutes a valid determination of $S_e$ and is not strongly affected by our lack of precise knowledge of the nuclear stopping at energies larger than 200 to 400 keV for nitrogen projectiles.

For the studies of the energy dependence of the range distributions it was tempting to determine the electronic stopping directly from the derivative function $dE/dR_p$. However, as just discussed, the energy region of 200 to 2000 keV is still low enough that the nuclear stopping is significant and must be taken into account. It is easy to invert the relation of Eq. (1) to find an expression for $S_e$ in terms of $dE/dR_p$:

$$S_e(E) = \frac{1}{N}\frac{dE}{dR_p}\left(1-\lambda_{\rm tr}^{-1}(E)R_p(E)\right)^{-1} - S_{n,\rm tr}(E)\,.$$

However, from studies of computer solutions for $R_p$ as a function of the projectile energy $E$ it was clear that very precise values for the derivative $dE/dR_p$ are needed to determine $S_e$ from this relation. Such precision cannot be claimed for our data. Thus, we resorted to the alternative of assuming a functional form for $S_e$:

$$S_e(E) = A(E/E_0)^p\,.$$

Using this form we have considered the two possibilities: determining both $A$ and $p$ by fitting the calculated values of $R_p$ to the data or determining $A$ alone with $p$ having a fixed value.

## III. RESULTS

### A. 800-keV $^{14}N^+$ implants in $Z_2$

We summarize our results for the range distributions of the 800-keV $^{14}N^+$ implants by showing in Fig. 1 the projected range and straggling in projected range as a function of target atomic number.

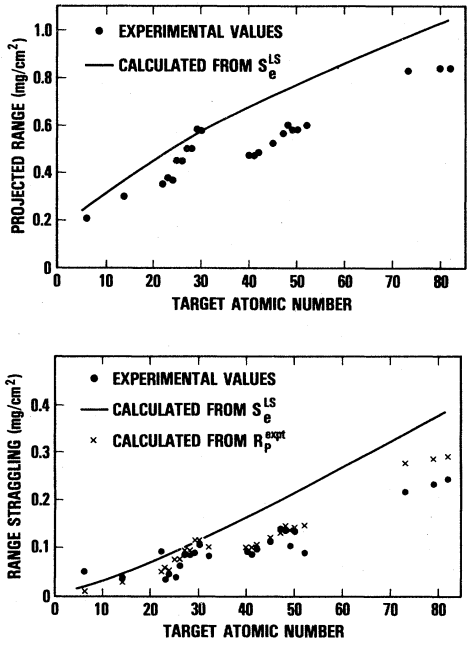


FIG. 1. Projected range (top) and straggling in projected range (bottom) vs. target atomic number for 800-keV $^{14}N^+$ ions. The solid circles show the results of the present experiment. The solid curves show values calculated from LSS transport theory with the LS values for $S_e$. The $x$'s (bottom) show the straggling calculated from LSS transport theory in which the values of $S_e$ inferred from the measured projected range were used. Slight irregularities in the solid curves which arise from the variation in the atomic weight of the target have been smoothed.

Shown for comparison are the corresponding results obtained from LSS transport theory in which the Lindhard-Scharff (LS) values[10] are used for the electronic stopping. The effects of the periodic structure in $S_e$ is clearly reflected in both $R_p$ and $\Delta R_p$. In addition, the values for the range straggling calculated from the LSS transport theory in which we took the experimentally inferred values for $S_e$ are also shown. It is clear that the use of the experimental electronic stopping gives rise to straggling which shows a closer correspondence with the data than the straggling which arises from use of the LS values. The experimentally inferred values for $R_p$ and $\Delta R_p$ are listed in Table I along with the values predicted from the LS electronic stopping and the values of $\Delta R_p$ obtained from $S_e^{expt}$. The third moments of the range distribution, $\Delta R_{3p}$, are also listed. These values, as discussed above, are to be regarded simply as parameters of the distributions and are used along with $R_p$ and $\Delta R_p$ to reconstruct the range distributions we inferred by using the inverse of the relations of Eq. (1).

TABLE I. Experimental (expt) and theoretical (LSS) values of the projected range $R_p$, range straggling $\Delta R_p$, and skewness $\Delta R_{3p}$, for 800-keV $^{14}N^+$ ions implanted in targets from carbon through lead. Also given are the values of straggling calculated (calc) from LSS theory in which the electronic stopping inferred from $R_p^{expt}$ is used. All values are in mg/cm².

| $Z_2$ | $R_p^{expt}$ | $R_p^{LSS}$ | $\Delta R_p^{expt}$ | $\Delta R_p^{calc}$ | $\Delta R_p^{LSS}$ | $\Delta R_{3p}^{expt}$ |
|---|---|---|---|---|---|---|
| 6 | 0.208 | 0.252 | 0.051 | 0.012 | 0.016 | +0.044 |
| 14 | 0.304 | 0.365 | 0.034 | 0.033 | 0.043 | −0.021 |
| 22 | 0.357 | 0.490 | 0.093 | 0.051 | 0.079 | −0.059 |
| 23 | 0.384 | 0.511 | 0.032 | 0.057 | 0.084 | +0.012 |
| 24 | 0.373 | 0.510 | 0.055 | 0.055 | 0.086 | −0.037 |
| 25 | 0.458 | 0.527 | 0.038 | 0.075 | 0.091 | −0.038 |
| 26 | 0.456 | 0.524 | 0.061 | 0.076 | 0.092 | −0.057 |
| 27 | 0.508 | 0.544 | 0.088 | 0.089 | 0.098 | −0.082 |
| 28 | 0.510 | 0.530 | 0.085 | 0.093 | 0.097 | −0.080 |
| 29 | 0.594 | 0.564 | 0.088 | 0.115 | 0.107 | −0.070 |
| 30 | 0.586 | 0.569 | 0.105 | 0.114 | 0.110 | −0.093 |
| 32 | 0.534 | 0.612 | 0.083 | 0.103 | 0.124 | −0.082 |
| 40 | 0.484 | 0.679 | 0.093 | 0.100 | 0.163 | −0.082 |
| 41 | 0.480 | 0.686 | 0.087 | 0.100 | 0.167 | −0.079 |
| 42 | 0.495 | 0.698 | 0.098 | 0.105 | 0.173 | −0.089 |
| 45 | 0.536 | 0.720 | 0.115 | 0.120 | 0.185 | −0.091 |
| 47 | 0.578 | 0.737 | 0.137 | 0.135 | 0.193 | −0.121 |
| 48 | 0.610 | 0.759 | 0.134 | 0.147 | 0.202 | −0.106 |
| 49 | 0.592 | 0.767 | 0.106 | 0.142 | 0.207 | −0.077 |
| 50 | 0.593 | 0.781 | 0.142 | 0.143 | 0.214 | −0.113 |
| 52 | 0.613 | 0.826 | 0.091 | 0.150 | 0.231 | −0.084 |
| 73 | 0.842 | 0.959 | 0.222 | 0.279 | 0.340 | −0.168 |
| 79 | 0.851 | 0.996 | 0.235 | 0.291 | 0.371 | −0.191 |
| 82 | 0.856 | 1.027 | 0.248 | 0.296 | 0.391 | +0.191 |

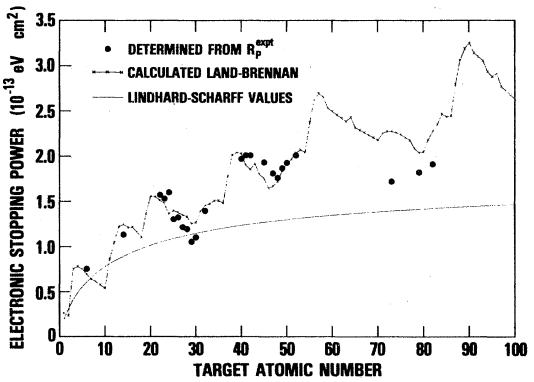


FIG. 2. Electronic stopping power vs target atomic number for nitrogen projectiles having velocity $v = v_0$. The solid circles show the values inferred from the projected range of 800-keV $^{14}N^+$ ions measured in the present experiment under the assumption of velocity-proportional electric stopping. The solid curve shows the LS values and the $x$-$x$-$x$ curve shows the values calculated by Land and Brennan (Ref. 6).

TABLE II. Values of the electronic stopping power at $v = v_0$ (350 keV) for $^{14}N$ in targets from carbon through lead as inferred from the projected range of 800-keV $^{14}N^+$ ions of this experiment. Values are given in units of $10^{-13}$ eV cm$^2$.

| $Z_2$ | $S_e^{expt}$ |
|---|---|
| 6 | 0.76 |
| 14 | 1.12 |
| 22 | 1.57 |
| 23 | 1.53 |
| 24 | 1.60 |
| 25 | 1.30 |
| 26 | 1.32 |
| 27 | 1.21 |
| 28 | 1.19 |
| 29 | 1.05 |
| 30 | 1.10 |
| 32 | 1.40 |
| 40 | 1.97 |
| 41 | 2.02 |
| 42 | 2.01 |
| 45 | 1.93 |
| 47 | 1.82 |
| 48 | 1.76 |
| 49 | 1.87 |
| 50 | 1.93 |
| 52 | 2.01 |
| 73 | 1.71 |
| 79 | 1.82 |
| 82 | 1.90 |

The values we have found for the electronic stopping power are shown in Fig. 2 and are listed in Table II. These values are given for incident nitrogen ions at the velocity $v = v_0$. Also shown in Fig. 2 are the values for $S_e$ calculated by Land and Brennan.[6] These calculations were performed with the Firsov model[18] modified so that Hartree-Fock atomic densities which reflect atomic structure replace the Thomas-Fermi densities of the original model. The Lindhard-Scharff values obtained from Thomas-Fermi atomic densities are also shown for comparison. The period structure clearly evident in the experimental data is on the average more closely fit with the use of the Hartree-Fock rather than the Thomas-Fermi atomic density in the calculation of $S_e$. These data show a minimum in the vicinity of copper which is deeper than the predictions of the theoretical models, a circumstance similar to the $Z_1$ oscillations in carbon.

### B. 200–2000 keV $^{14}N^+$ implants in Fe, Ni, and Zr

The range distributions for the 200–2000-keV $^{14}N^+$ implants in iron, nickel, and zirconium are summarized in Fig. 3 where we show the projected range and straggling as a function of the nitrogen-ion velocity. For completeness we also show the values for incident nitrogen at lower energies, 25–150 keV. This work is discussed elsewhere.[4] These data are compared to results obtained from the LSS transport theory by assuming the electronic stopping is velocity proportional, $S_e = v/v_0$, and by adjusting the constant $A$ so that the calculated values for $R_p$ agree with the experimental values in a least-squares sense in the energy region from 200 to 2000 keV only. We see from Fig. 3 close agreement for all targets between the experimental values and the theoretical curve for $R_p$ throughout the entire energy region considered and reasonable consistency for $\Delta R_p$. There is, however, a clear and persistent tendency for all targets for the straggling data to lie above the theoretical curve at low velocities and to fall below at high velocities. The former behavior which produces the larger widths for the distributions is not surprising, especially at low velocities where the system resolution, relative to the widths of the distributions, is poorer. However, we have no explanation for the behavior at higher velocities. This behavior could be related to a need either for a different energy dependence of electronic stopping or for a different differential cross section for the nuclear stopping.

In order to investigate the energy dependence of $S_e$, we have considered a more general analytic form for $S_e$. As discussed above, we cannot determine $S_e$ directly from the derivative $dE/dR_p$. The dependence most frequently assumed is $S_e = A(E/E_0)^p$. We determined the constants by employing least-squares fits of the projected range data to the values calculated from Eq. (2) where both $A$ and $p$ are varied and where $A$ alone is varied with $p$ fixed at 0.4, 0.5, and 0.6. For any given target and for $p$ assuming its fixed values, $A$ was

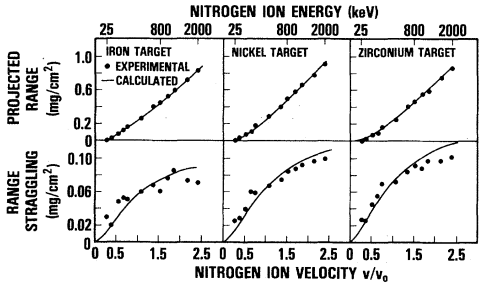


FIG. 3. Projected range and range straggling vs nitrogen-ion velocity for $^{14}N^+$ ions in iron, nickel, and zirconium targets. The solid circles show the values measured in the present experiment. The solid curves show results calculated from LSS transport theory in which velocity-proportional electronic stopping adjusted for a least-squares fit of the projected range is used.

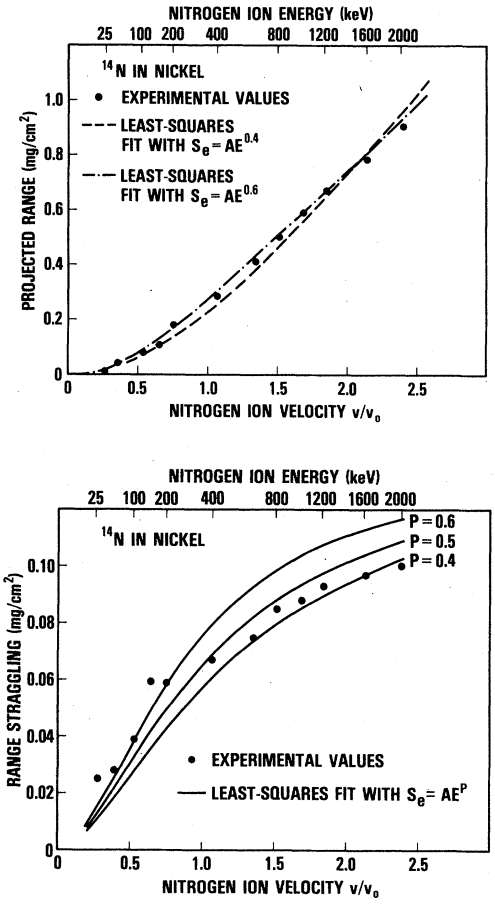


FIG. 4. Projected range (top) and range straggling (bottom) vs nitrogen-ion velocity for $^{14}N^+$ ions in nickel. The solid circles show the values obtained in the present experiment. The curves show results calculated from LSS transport theory in which the electronic stopping is given by the form $S_e = A(E/E_0)^p$ with $p = 0.4$, 0.5, and 0.6 and $A$ determined by a least-squares fit of the projected range. (The curve for $p = 0.5$ for the projected range falls between the $p = 0.4$ and 0.6 curves and is not shown.)

found to vary by no more than about 10%. For the case of velocity-proportional stopping ($p = 0.5$) where $A$ is determined from the single measurement at 800 keV or from the complete data set, $A$ varies by no more than 5%. Thus, if we assume velocity proportionality, we arrive at similar results for the electronic stopping even if $S_e$ is inferred from the measured $R_p$ at a single energy only. However, if the value of the exponent $p$ is also varied, we find a range $p = 0.56$ to $p = 0.64$ for these three targets.

In Fig. 4 we show plots of $R_p$ and $\Delta R_p$ for a single target, nickel, as calculated for fixed values of $p$ from 0.4 to 0.6. We see that the projected range is not a sensitive function of $p$; that is, $R_p$ is not sensitive to the details of the energy dependence of the electronic stopping power. On the other hand, the straggling, $\Delta R_p$, is somewhat more sensitive. The data lie closer to the $p = 0.4$ curve at higher energies but favor the $p = 0.6$ curve at lower energies. However, for all targets the behavior at higher energies, having $p$ between 0.4 and 0.5, contrasts with the results from the least-squares fit of $R_p$ where $p$ took values lying about 0.6. We must conclude that the present data do not specify uniquely the energy dependence for $S_e$. However, the results are consistent with velocity proportionality. In addition, the general behavior which we have discussed for the nickel target holds for the iron and zirconium targets also, and hence we conclude that the energy dependence of $S_e$ does not depend strongly on the target material.

### C. 200- and 400-keV atomic and molecular N implants

A part of the present study was to compare implant distributions arising from incident beams of atomic or molecular nitrogen at equal energy per atom to see if there is a difference. The results are summarized in Table III. Also given are the results for incident nitrogen at lower energies, 25 to 100 keV per atom. At the higher energies we

TABLE III. Experimental values for the projected range and range straggling for atomic and nitrogen of equal energy per atom in targets of iron, nickel, zirconium, and gold. All values are given in mg/cm$^2$.

| Target | Energy per atom (keV) | $R_p$ | | $\Delta R_p$ | |
|---|---|---|---|---|---|
| | | $N^+$ | $N_2^+$ | $N^+$ | $N_2^+$ |
| Fe | 25 | 0.001 | 0.001 | 0.029 | 0.028 |
| | 50 | 0.035 | 0.035 | 0.020 | 0.020 |
| | 100 | 0.075 | 0.089 | 0.048 | 0.033 |
| | 200 | 0.163 | 0.155 | 0.051 | 0.054 |
| | 400 | 0.265 | 0.271 | 0.060 | 0.061 |
| Ni | 25 | 0.013 | 0.016 | 0.025 | 0.020 |
| | 50 | 0.048 | 0.042 | 0.028 | 0.026 |
| | 100 | 0.086 | 0.090 | 0.039 | 0.041 |
| | 200 | 0.188 | 0.174 | 0.059 | 0.059 |
| | 400 | 0.319 | 0.298 | 0.067 | 0.065 |
| Zr | 25 | 0.001 | 0.016 | 0.034 | 0.027 |
| | 50 | 0.036 | 0.038 | 0.032 | 0.029 |
| | 100 | 0.073 | 0.076 | 0.045 | 0.046 |
| | 200 | 0.171 | 0.142 | 0.070 | 0.064 |
| | 400 | 0.269 | 0.261 | 0.072 | 0.081 |
| Au | 25 | 0.014 | 0.015 | 0.023 | 0.068 |
| | 50 | 0.015 | 0.064 | 0.093 | 0.087 |
| | 100 | 0.145 | 0.098 | 0.114 | 0.110 |
| | 200 | 0.253 | 0.237 | 0.154 | 0.172 |
| | 400 | 0.459 | 0.436 | 0.207 | 0.232 |

find systematic differences with the molecular implants being slightly more shallow, one exception being the case of 400 keV per atom N in iron. The difference is about 5% at these energies. The widths are comparable. At the lower energies no systematic trend can be detected. However, as we have discussed elsewhere,[4] the existence of a front surface peak coupled with the relatively broad resonance width makes the determination of $R_p$ and $\Delta R_p$ from these data ambiguous, and small differences between the atomic and molecular implants would be difficult to discern. We have previously discussed possible origins of the difference observed in terms of correlated molecular-cluster effects and concluded that these cannot explain the 5% effect observed.[19] Our general conclusion is that the molecular incident beam may give rise to more shallow implant distributions of the order of a few percent but that additional experimental work is required before definitive results can be obtained.

## IV. DISCUSSION

We have performed an extensive study of the behavior of range distributions for nitrogen ions implanted in solid targets at energies from 25 to 2000 keV. From studies of the energy dependence of the range distributions we conclude that the electronic stopping power for $N^+$ projectiles is consistent with the relation $S_e = A(E/E_0)^{1/2}$ throughout the energy region considered. Thus we have used velocity-proportional electronic stopping to infer $S_e$ for N projectiles from the measured projected range at a single projectile energy, 800 keV. Our choice of targets of iron, nickel, and zirconium was made on the basis of having one target near the minimum, one near the maximum, and one at the midpoint on the stopping-power curve. There is no indication that the energy dependence of the stopping depends significantly on the target material.

From our studies of the range distributions as a function of target material we have shown the periodic structure of $S_e$ in $Z_2$ for nitrogen as a projectile. This has been done in detail now in two regions, $Z_2 = 22$ to $Z = 32$ and $Z = 40$ to $Z = 52$. The theoretical models for $S_e$ in general predict broad minima centered about those elements for which a $d$ shell closes. This can be seen from the calculations of Land and Brennan in Fig. 2. Our data show this feature in the vicinity of copper where the $3d$ shell closes, and in the vicinity of palladium, where the $4d$ shell closes. A similar minimum should exist near gold where the $5d$ shell closes. The present data, which are rather incomplete in this region, may raise a question concerning this minimum. It would be of considerable interest to extend the present results to include at least the $Z_2$ region from hafnium ($Z_2 = 72$) to lead ($Z_2 = 82$). Another region of similar interest lies about ytterbium ($Z_2 = 70$) where the $4f$ shell closes. Theory predicts a small minimum here.

As a general conclusion concerning the range distributions we find that the LSS transport theory correlates well with the data if accurate values for the electronic stopping are used in the theory. That is, we have used the experimentally determined first moment of the distribution to infer the electronic stopping power under the assumption that $S_e$ is velocity proportional. The second moments that result from the use of these values of $S_e$ within the LSS theory generally agree well with the measured values over the range of $Z_2$ we studied. The third moment of the range distribution is not well determined from our data analysis. However, this moment (skewness) exerts only a minimal influence on the distributions at the higher energies where $\Delta R_p$ is much less than $R_p$.

It is of interest to compare our values for the electronic stopping with those of Porat and Ramavataram.[20] These authors have determined $S_e$ by measuring the energy loss of nitrogen ions through thin foils of C, Al, Ni, Ag, and Au at energies from 400 keV to roughly 4 MeV. Because Al and Si are adjacent in the periodic table and the modified Firsov calculation predicts similar values, we have compared our result for Si directly with the Porat-Ramavataram results for Al. For the carbon target we find differences of about 10%. This is not surprising as the stopping powers especially for carbon targets are known to depend sensitively on the chemical form of the target. For the remaining elements the two sets of measurements agree within a few percent.

## ACKNOWLEDGMENTS

The authors wish to thank P. K. Cady and J. Mays for their assistance in taking the measurements of the $\gamma$-ray yield. This research was sponsored by the Naval Surface Weapons Center, Independent Research Program.

*Also Catholic University of America, Washington, D.C. 20017.

[1]D. G. Simons, D. J. Land, J. G. Brennan, and M. D. Brown, Phys. Rev. A 12, 2383 (1975).

[2]D. G. Simons, D. J. Land, J. G. Brennan, and M. D. Brown, in *Ion Beam Surface Layer Analysis*, edited by O. Meyer, G. Linker, and F. Käppeler (Plenum, New York, 1976), pp. 863 and 851; in *Ion Implantation in Semiconductors and Other Materials*, edited by F. Chernow, J. A. Borders, and D. K. Brice (Plenum, New York, 1977), p. 703.

[3]J. G. Brennan, D. J. Land, M. D. Brown, and D. G. Simons, Nucl. Instrum. Methods 149, 143 (1978).

[4]D. J. Land, D. G. Simons, J. G. Brennan, and M. D. Brown, Radiat. Eff. (to be published).

[5]D. J. Land and J. G. Brennan, Nucl. Instrum. Methods 132, 89 (1976); D. J. Land, J. G. Brennan, D. G. Simons, and M. D. Brown, Phys. Rev. A 16, 492 (1977).

[6]D. J. Land and J. G. Brennan, At. Data Nucl. Data Tables 22, 235 (1978).

[7]J. Lindhard, M. Scharff, and H. E. Schiött, K. Dan. Vidensk. Selsk. Mat. Fyz. Medd. 33, No. 14 (1963).

[8]W. K. Chu and D. Powers, Phys. Rev. 187, 478 (1969); C. C. Rousseau, W. K. Chu, and D. Powers, Phys. Rev. A 4, 1006 (1971); F. Bernhard, U. Müller-Jareis, G. Rockstroh, and S. Schwabe, Phys. Status Solidi 35, 285 (1969); P. Apel, U. Müller-Jareis, G. Rockstroh, and S. Schwabe, Phys. Status Solidi A 3, K173 (1970); W. Pietsch, U. Hauser, and W. Neuwirth, Nucl. Instrum. Methods 132, 79 (1976).

[9]J. H. Ormrod and H. E. Duckworth, Can. J. Phys. 41, 1424 (1963); J. H. Ormrod, J. R. MacDonald, and H. E. Duckworth, *ibid.* 43, 275 (1965); J. R. MacDonald, J. H. Ormrod, and H. E. Duckworth, Z. Naturforsch. A27, 130 (1966); B. Fastrup, P. Hvelplund, and C. A. Sautter, K. Dan. Vidensk. Selsk. Mat. Fyz. Medd. 35, No. 10 (1966); P. Hvelplund and B. Fastrup, Phys. Rev. 165, 408 (1968); B. Fastrup, A. Borux, and P. Hvelplund, Can. J. Phys. 46, 489 (1968); P. Hvelplund, K. Dan. Vidensk. Selsk. Mat. Fyz. Medd. 38, No. 4 (1971); D. Ward *et al.*, Can. J. Phys. 57, 645 (1979).

[10]J. Lindhard and M. Scharff, Phys. Rev. 124, 128 (1961).

[11]W. Brandt, A. Ratkowski, and R. H. Ritchie, Phys. Rev. Lett. 33, 1325 (1976); D. S. Gemmell, J. Remillieux, J. C. Poizat, M. J. Gaillard, R. E. Holland, and Z. Vager, Nucl. Instrum. Methods 132, 61 (1976).

[12]A. V. Nero, Nucl. Phys. A185, 213 (1972).

[13]D. J. Land, D. G. Simons, J. G. Brennan, and M. D. Brown, Fourth International Conference on Ion Beam Analysis, Aarhus, Denmark, 1979 (unpublished).

[14]H. H. Andersen and J. F. Ziegler, *Hydrogen, Stopping Powers and Ranges in All Elements* (Pergamon, New York, 1977).

[15]J. F. Gibbons and S. Mylroie, Appl. Phys. Lett. 22, 563 (1973).

[16]K. B. Winterbon, *Ion Implantation Range and Energy Deposition Distributions Vol. 2, Low Incident Ion Energies* (Plenum, New York, 1975).

[17]M. Luomajärvi, J. Keinonen, M. Bister, and A. Anttila, Phys. Rev. B 18, 4657 (1978).

[18]O. B. Firsov, Zh. Eksp. Teor. Fiz. 36, 1517 (1959) [Sov. Phys.—JETP 9, 1076 (1959)].

[19]D. G. Simons, D. J. Land, J. G. Brennan, and M. D. Brown, in *Proceedings of the Fourth Conference on the Scientific and Industrial Application of Small Accelerators*, edited by J. Duggan and I. L. Morgan (IEEE, New York, 1976), p. 568.

[20]D. I. Porat and K. Ramavataram, Proc. Phys. Soc. London 78, 1135 (1961).